Strong Nonlinear Optical Effects from a New Polymeric Silver(I)–Propyl–Benzotriazole Complex

Hong Xu,[1] Yinglin Song,[2] Xiangru Meng,[1] Hongwei Hou,[1] Yaoting Fan[1]

[1]*Department of Chemistry, Zhengzhou University, Henan 450052, People's Republic of China*
[2]*Department of Physics, Suzhou University, Suzhou 15008, People's Republic of China*

Received 6 May 2010; accepted 6 May 2011
DOI 10.1002/app.34872
Published online 27 December 2011 in Wiley Online Library (wileyonlinelibrary.com).

ABSTRACT: A new polymeric Ag(I) complex $\{[Ag_2(pbbt)_3](NO_3)_2{\cdot}0.5H_2O\}_n$ [where pbbt = 1,1′-(1,3-propylene)-bis-1H-benzotriazole] was synthesized as a good optical limiter. Single-crystal X-ray diffraction determined that the complex assumed a rare, two-dimensional lamellar structural motif with isolated cavities of $[Ag_6(pbbt)_6]$. The *Z*-scan measurements of an 8-ns pulsed laser at 532 nm revealed that the presented complex in dimethylformamide exhibited very strong third-order optical nonlinear absorption. The optical-limiting (OL) performance was investigated in the sample of the complex induced by 8-ns and 30-ps pulses at 532 nm. The results show that this complex exhibited large OL effects with a very low limiting threshold value of 0.16 J/cm^2 under 8-ns pulse and 0.56 J/cm^2 under 30-ps pulses, among those of the best OL materials. Density functional theory calculation results further confirmed the cooperative contributions of Ag ions and bridge ligands to the optical nonlinearities of Ag(I)-containing metal–organic complex. J Appl Polym Sci 125: 682–689, 2012

Key words: metal–polymer complexes; NLO; nonlinear polymers; structure

INTRODUCTION

Along with the rapid development of new lasers with shorter pulses, higher peak intensities, and tunable wavelengths, optical-limiting (OL) materials have generated much interest for their applications in protecting human eyes and sensors from intense optical beams.[1–3] As promising OL materials, inorganic semiconductors, organic materials, nanoparticles, metallophthalocyanine complexes, and fullerene and its derivatives have been studied extensively. Still, each class has its own merit and limitation. For example, although fullerene is a prominent OL material, its poor solubility is a serious shortcoming and, thus, hinders its promise for OL use. Therefore, current research in this field depends critically on the development of new OL materials.

Metal–organic complexes were originally found to present low nonlinear optical (NLO) activity at the end of the 1980s and, thus, were mainly academic curiosities. In recent decades, however, metal–organic complexes were found to have various kinds of fantastic structures, many of which possess potential applications, including as potential OL materials.[4–6] The most promising feature in metal–organic complexes is the opportunity provided to modify and optimize their building blocks at the molecular level for the design of highly active OL-phores. In previous works, we investigated some Ag-containing complexes with enhanced OL properties, including the polymeric complexes $\{[Ag(bpfp)](NO_3)(H_2O)\}_n$ (where bpfp is *N*,*N*′-bis(3-pyridylformyl) piperazine) and $\{[Ag(btx)](NO_3)H_2O\}_n$ [where btx is 1, 4-bis(triazol-1-ylmethyl) benzene],[7] the cluster $Ag_{10}(dcapp)_4]{\cdot}2(OH){\cdot}12H_2O$ (where H_2dcapp is 2,6-dicarboxamido-2-pyridylpyridine),[8] and the one-dimensional polymeric cluster $\{[AgI(inh)]_6(KI)\}_n$ (where inh is N-(isonicotinoyl)-N-nicotinoylhydrazine),[9] all of which showed interesting and strong OL effects. To develop this promising field and also to search for better OL materials, we herein present our studies on the structural and NLO properties of a new metal–organic polymeric complex $\{[Ag_2(pbbt)_3](NO_3)_2{\cdot}0.5H_2O\}_n$ (where pbbt = 1,1′-(1,3-propylene)-bis-1H-benzotriazole) (**1**). The complex showed large OL capabilities, both toward nanosecond and picosecond pulses on the basis of cubic NLO properties. By density functional theory (DFT) calculation and comparing this complex to the pure ligand pbbt, we gleaned some information about the relationship between the structure and NLO properties (Scheme 1).

Additional Supporting Information may be found in the online version of this article.

Correspondence to: H. Hou (houhongw@zzu.edu.cn).

Contract grant sponsor: Education Department of He'nan Province; contract grant number: 2010A150025.

Contract grant sponsor: Science and Technology Projects of Zhengzhou 27 District; contract grant number: 20103376.

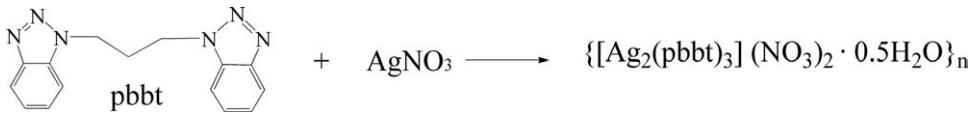

Scheme 1

EXPERIMENTAL

Materials and physical techniques

All chemicals, such as silver nitrate (>99%, Aldrich, CAS 7761-88-8), were of reagent-grade quality, were obtained from a commercial source, and were used without further purification. 1,3-Dibromopropane (>99%, Aldrich, CAS 109-64-8) and 1H-benzotriazole (≥98.0%, Fluka, no. 12799) were used to prepare the ligand pbbt. The synthesis of the ligand pbbt was performed according to literature methods.[10] IR data was recorded on a Nicolet NEXUS 470 Fourier transform infrared spectrophotometer with KBr pellets in the 400–4000-cm^{-1} region. An ultraviolet–visible (UV–vis) spectrum was obtained on an HP 8453 spectrophotometer (Hewlett-Packard Company, California). Elemental analysis (C, H, and N) was carried out on a FLASH EA 1112 elemental analyzer.

Synthesis of $\{[Ag_2(pbbt)_3](NO_3)_2 \cdot 0.5H_2O\}_n$

A solution of pbbt (14.6 mg, 0.05 mmol) in 5 mL of MeOH was slowly added to a 2-mL H_2O solution of $AgNO_3$ (8.5 mg, 0.05 mmol). The resultant solution was allowed to stand at room temperature in the dark at once. Colorless transparent crystals grew within 2 months at room temperature:

Yield = 55%. Calcd for $C_{45}H_{43}Ag_2N_{20}O_{6.5}$: C, 45.58%; H, 3.69%; N, 23.84%. Found: C, 45.72%; H, 3.67%; N, 23.71%. IR (KBr, cm^{-1}): 3031m, 1619w, 1491w, 1450m, 1327s, 751s.

Structural determination

The crystal data and experimental details for this complex are contained in Table I. Suitable single crystals with dimensions of 0.30 × 0.22 × 0.20 mm^3 for this complex were selected for single-crystal X-ray diffraction analysis. Data collection was performed on a Rigaku RAXIS-IV (Osaka, Japan) image plate area detector for study with graphite–monochromated Mo–Kα (λ = 0.71073 Å) radiation at 291(2) K with the ω–2θ scan technique. The data was corrected for Lorentz and polarization factors and for absorption with empirical scan data. This structure was solved with the SHELXL program[11] and was refined by full-matrix, least-squares methods based on F^2, with anisotropic thermal parameters for the nonhydrogen atoms. The hydrogen atoms were located theoretically and were not refined. Crystal data and structural refinement of the structure are summarized in Table I. Selected bond lengths and bond angles of this complex are listed in Table II. The Cambridge Crystallographic Data Centre number of this complex is 212227. The data can be obtained free of charge via www.ccdc.cam.ac.uk/conts/retrieving. html (or from the Cambridge Crystallographic Data Centre, 12, Union Road, Cambridge CB21EZ, United Kingdome, fax: (44)1223-336-033, deposit@ccdc.cam. ac.uk).

Linear absorption spectra measurements

UV–vis absorption spectra of dimethylformamide (DMF) solutions of this complex and pbbt were recorded, ranging from 250 to 800 nm, on a Jasco V-550 UV–vis spectrophotometer (Connecticut).

Molecular weight measurements

The molecular weight and molecular weight distribution of this complex were determined at 40°C with gel permeation chromatography (GPC; Waters Associates model HPLC/GPC 515 liquid chromatograph (Milford, MA), equipped with a refractive-index detector and μ-Styragel columns and calibrated with standard polystyrene), with DMF as the eluent and a flow rate of 1.0 mL/min.

Third-order NLO property measurements

The third-order NLO property of this complex was evaluated by the *Z*-scan technique in DMF solution

TABLE I
Crystal and Structure Refinement Data for $\{[Ag_2(pbbt)_3](NO_3)_2 \cdot 0.5H_2O\}_n$

Formula	$C_{45}H_{43}Ag_2N_{20}O_{6.50}$
Formula weight	1183.73
Color	Colorless
Crystal system	Rhombohedral
Space group	*R*3c
a (Å)	14.406(2)
b (Å)	14.406(2)
c (Å)	40.948(8)
α (°)	90
β (°)	90
γ (°)	120
Volume ($Å^3$)	7359.5(21)
Z	6
D_c (g/cm^3)	1.603
Absorbance coefficient (mm^{-1})	0.870
F(000)	3594
Collected/unique reflections	2195/1755
Goodness of fit on F^2	1.159
Final *R* indices	$R_1 = 0.0741$
$[I > 2\sigma(I)]$	$wR_2 = 0.0493$

TABLE II
Selected Bond Lengths (Å) and Angles (°) for $\{[Ag_2(pbbt)_3](NO_3)_2{\cdot}0.5H_2O\}_n$

Ag1–N1	2.176(10)	Ag2–N6	2.432(7)
Ag1–N1#1	2.176(10)	Ag2–N6#3	2.432(7)
Ag1–N1#2	2.176(10)	Ag2–N6#4	2.432(7)
N1–Ag1–N1#2	106.6(4)	N6 #3–Ag2–N6#4	103.3(2)
N1#2–Ag1–N1#1	106.6(4)	N6–Ag2–N6#4	103.3(2)

Symmetry transformations used to generate equivalent atoms: #1 $-x+y+1, -x+1, z$ #2 $-y+1, x-y, z$ #3 $-x+y, -x, z$ #4 $-y, x-y, z$.

(1.4×10^{-4} mol/dm^3). The dilute DMF solution was placed in a 1-mm quartz cuvette for NLO measurement. The nonlinear refraction and nonlinear absorption were measured with a linearly polarized laser light ($\lambda = 532$ nm; pulse width = 8 ns) generated from a Q-switched and frequency-doubled Nd:YAG laser with a repetition rate of 2 Hz. The spatial profiles of the optical pulses were nearly Gaussian. The laser beam was focused with a 25-cm focal-length focusing mirror. The radius of the beam waist was measured to be 35 ± 5 μm (half-width at $1/e^2$ maximum). The interval between the laser pulses was chosen to be about 5 s for operational convenience. The incident and transmitted pulse energies were measured simultaneously by two Laser Precision detectors (RjP-735 energy probes) (Geomaster Group, Tianji, china), which were linked to a computer by an IEEE interface. The third-order NLO property of the sample was manifested by movement of the samples along the axis of the incident beam (*Z* direction) with respect to the focal point.[12] An aperture of 0.5 mm in radius was placed in front of the detector to assist in the measurement of the self-focusing effect.

OL effect measurements

The OL measurements of this complex and pbbt in DMF solution (the same concentrations as those in the third-order NLO measurements) were performed with linearly polarized 8-ns and 30-ps durations at 532 nm generated from a Q-switched frequency-doubled Nd:YAG laser and a mode-locked, frequency-doubled Nd:YAG laser, respectively. The spatial profiles of the optical pulses were of nearly Gaussian transverse mode. The pulsed laser was focused onto the sample cell with a 30-cm focal-length mirror. The spot radius of the laser beam was measured to be 55 μm (half-width at $1/e^2$ maximum). The energy of the input and output pulses were measured simultaneously by precision laser detectors (Rjp-735 energy probes), which were linked to a computer by an IEEE interface,[13] whereas the incident pulse energy was varied by a Newport Co. attenuator (UK). The interval between the laser pulses was chosen to be 1 s to avoid the influence of thermal and long-term effects.

Computational methods

DFT has been proven to be extremely useful in treating metals when the requirements of both accuracy and computing economy are considered.[14–16] The DFT B3LYP method is always the method of choice to deal with complicated systems containing transition metals and has been used to reveal the structure–NLO property relationships for many metal–organic complexes.[7,8,14–17] Hence, in this work, the DFT/B3LYP method was adopted. On the basis of the crystal structure, a B3LYP exchange-correlation functional was carried out for the molecular orbital of $[Ag(pbbt)_3]^+$ segment of Ag1 and Ag2, respectively. The calculations were carried out with a mix basis set, that is, a 6-311G** basis set for C, N, and H atoms, LanL2DZ, which had a relativistic effective core potential with a valence basis set, for Ag atoms. The calculation continued until the root mean square gradient was less than 0.162 kcal/mol. All of the theoretical calculations were carried out with the Gaussian 03 program package.[18]

RESULTS AND DISCUSSION

The reaction of $AgNO_3$ and pbbt in a metal-to-ligand ratio of 2 : 1 in a mixed MeOH–H_2O solution gave rise to this complex. As depicted in Figure 1, the complex presented a rare lamellar structural motif[19] with isolated cavities of $Ag_6(pbbt)_6$. Each Ag ion was trigonally coordinated by three nitrogen atoms from different pbbt ligands, which were symmetry equivalent and were related by a threefold axis passing through the Ag center. There were two crystallographically independent Ag ions [Ag1 and Ag2]. The Ag1—N bond lengths were 2.176(10) Å, and the bond angles around Ag1 were 106.6(4)°. The dihedral angle between two benzotriazole planes from the same pbbt was 45.0°. Three nitrogen atoms from three pbbt ligands coordinated Ag1 to form a standard pyrometric cone, in which nitrogen atoms were located in a trigonal plane geometry, and the Ag1, which was at 1.142 Å up the trigonal plane, occupied the apical position. The coordination environment around Ag2 was similar to that of Ag1, but the Ag2—N bond lengths of 2.432(7) Å were longer than those of Ag1—N, and the bond angles around Ag2 [103.3(2)°] were different from those around Ag1 as well. Ag2 was 0.7858 Å down the trigonal plane formed by three nitrogen donors. Disorder occurred in the pbbt ligands. Continual symmetry operations about the threefold axes passing through the two center Ag ions yielded a two-dimensional network composed of the repeating unit $[Ag_6(pbbt)_6]$ with a hexagonal conformation. There was a crystallographic C_3 symmetry axis passing through its center in each $Ag_6(pbbt)_6$ unit, where the distance between

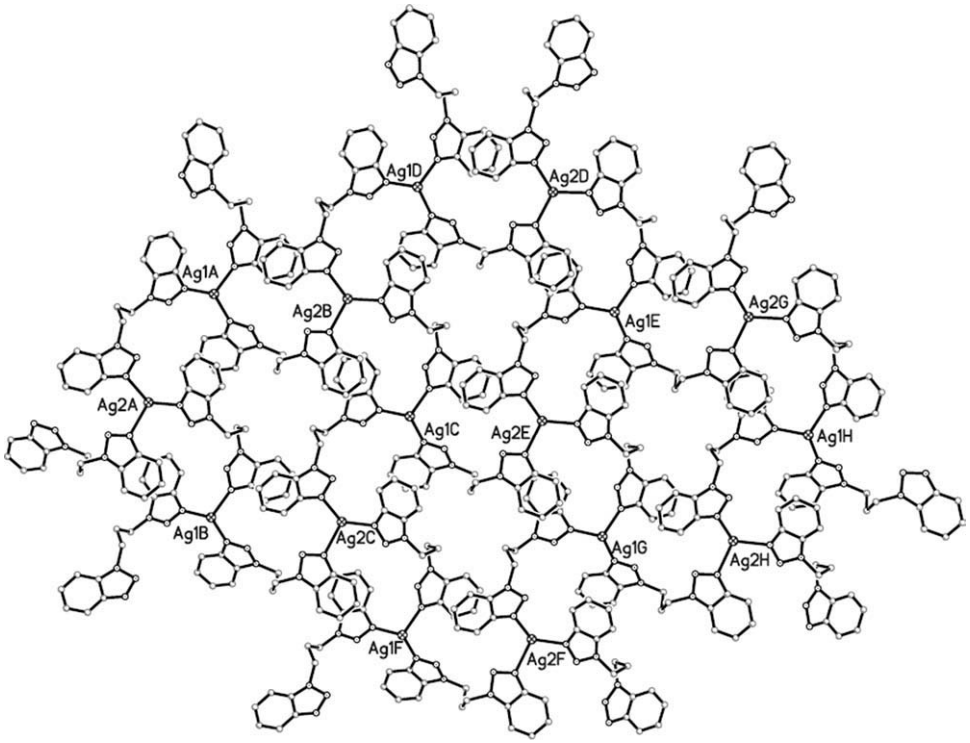

Figure 1 Two-dimensional structure of $\{[Ag_2(pbbt)_3](NO_3)_2 \cdot 0.5H_2O\}_n$ with hexagonal-shaped units (NO_3^- was deleted for clarity).

two adjacent Ag ions was 8.330 Å with an Ag···Ag···Ag angle of 119.7°, and the six Ag ions were nearly coplanar (the mean deviation from the plane was 0.2344°).

The linear absorption spectra of the presented complex and pbbt in DMF solution are reported in Figure 2. From the figure, it can be seen that the maximum of the absorption peak of this complex was positioned at 288 nm, which was redshifted compared to that of the free pbbt (279 nm). It could be associated with the metal and ligand charge transfer.[20] Also, the spectra of this complex showed additional, very weak absorption bands around 380 nm; these were tentatively assigned as ligand–localized transitions.[21,22] In the absorption spectra, the weak ground-state absorption in the visible and near-infrared regions suggested that the wavelength of the laser light (532 nm) was within the nonresonant absorption region.

The molecular weight of this complex was determined in DMF solution by GPC. GPC analysis revealed that the number-average molecular weight was 120,782 and that the weight-average molecular weight was 145,291. The result indicates that the dissolved complex was polymeric, existed in pieces of the same size, and afforded stable oligomers with a molar mass of approximately 1200 g/mol. It was similar to reported metal–organic polymers.[23,24]

The effective third-order NLO absorptive and refractive properties of the investigated complex were recorded by the *Z*-scan technique. The results are shown in Figure 3. In the figure, a reasonable fit between the experimental data and the theoretical curve (solid curve) suggests that the experimentally obtained NLO effects were effectively third order in nature. The filled squares are the experimental data, and the solid line is the theoretical curve from eqs. (1)–(5).

The nonlinear absorptive property is depicted in Figure 3(a) by the *Z*-scan technique under an open-aperture configuration with a pulse width of 8 ns at 532 nm and 2-Hz repetition rate. The NLO absorption performance of the investigated polymer could be presented by the following equations:

$$T(Z) = \frac{1}{\sqrt{\pi} q(Z)} \int_{-\infty}^{+\infty} \ln [1 + q(Z)] e^{\tau^2} d\tau \qquad (1)$$

$$q(Z) = \int_0^{\infty} \int_0^{\infty} \alpha_2 \frac{I_0}{1 + (Z/Z_0)^2} e^{[-2(\gamma/\omega_0)^2 - (t/t_0)^2]} \frac{1 - e^{-\alpha_0 L}}{\alpha_0} r dr dt \qquad (2)$$

where $T(z)$ represents the transmittance, which is defined here as the ratio of the transmitted pulse energy to the incident pulse energy at 532 nm; Z is the distance of the sample from the focal point; $Z_0 = \pi(\omega_0)^2/\lambda$ with ω_0 being the spot radius of the laser beam at focus and λ being the wavelength of the laser. $q(Z)$ is represented by equation (2). $I(z)$ is the

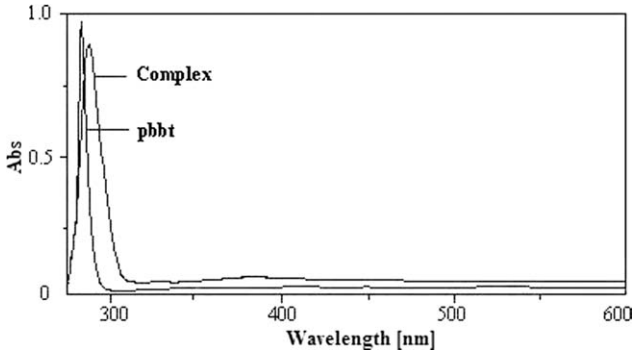

Figure 2 UV–vis spectra of $\{[Ag_2(pbbt)_3](NO_3)_2{\cdot}0.5H_2O\}_n$ and pbbt in a 1.4×10^{-4} mol/dm^3 DMF solution. Abs = absorbance.

incident light irradiance (I_0 is the peak irradiation intensity at focus, here $I_0 = 8.2 \times 10^8$ w/cm^2); α_0 and α_2 denote the linear and nonlinear absorption coefficients, respectively; r is the radial coordinate; T and t are the time; t_0 is the pulse width; L is the optical path ($L = 0.5$ cm in these experiments). As shown in Figure 3(a), the absorption increased as $I(z)$ increased. The normalized transmittance (T) dropped to about 82% at the focus; this showed a strong NLO absorptive effect. The best fits of eqs. (1) and (2) to the open-aperture configuration of Figure 3(a) gave an effective α_2 value of 3.20×10^{-8} m/W.

The effective third-order NLO susceptibility [$|\chi^{(3)}|$] value of the investigated complex was 1.05×10^{-8} esu, which was determined by the subtraction of the relatively weak background noise and the contribution of the solvent by comparison of the signal intensity with that of CS_2 (the $|\chi^{(3)}|$ value of CS_2 was taken to be 6.8×10^{-13} esu under the same experimental conditions). Also, we could use the hyperpolarizability (γ) to represent the NLO properties of the neat materials

$$\gamma = \chi^{(3)}/NF^4$$

where N is the number density of a present complex in the sample (cm^{-3}) and F is the local field correction factor $\{F = [(n^2+2)/3]\}$. Because the investigated sample was very dilute, n was regarded as the index of refraction of the solvent, and F^4 was calculated to be 3 in this work. Thus, γ for the complex was calculated to be 4.15×10^{-26} esu. The two data revealed that the polymeric Ag(I) complex possessed very strong nonlinear absorption, giving rise to larger $\chi^{(3)}$ and γ values than many well-known NLO materials, such as C_{60},[25] inorganic semiconductors,[26] and metal clusters.[27]

To verify whether silver ions were in the active role of the NLO properties, we measured the third-order NLO absorptive and refractive characteristics of the pure ligand pbbt at a wavelength of 532 nm in dilute DMF solution (1.4×10^{-4} mol/dm^3). The result shows that the ligand did not perform nonlinear absorptive properties, and no detectable valley or peak in the open-aperture curve was observed at 532 nm for pbbt. Obviously, the incorporation of metal Ag ions led to a dramatic increase in the NLO response, in marked contrast to the behavior of the related pure organic ligand. Also, the investigated complex possessed much stronger NLO capabilities than Zn(II), Ni(II), and Co(II) polymeric complexes based on pbbt (their $|\gamma|$ values were $\sim \times 10^{-29}$ esu).[28,29] This could have been due to the excellent electroconductivity and photoluminescent properties, Ag ions act as connectors to extend frameworks and furnish effective pathways for electronic conductivity in polymeric complex chromophores.[30,31] Therefore, Ag-containing complexes are usually found to exhibit very large third-order NLO effects.[8,9,27,32] Also, the large value of $\chi^{(3)}$ of this complex mostly depended on its large $Im\chi^{(3)}$, namely, α_2. Thus, the presence of a strong NLO absorption effect significantly enhanced the overall OL performance of the complex.

With regard to the sufficiently strong nonlinear absorption of the investigated complex, its OL measurement was performed in the open-aperture configuration. Such a configuration allowed for the determination of the NLO effects associated solely with changes of α_2. It should be pointed out that our measurement of the transmitted pulse energy was conducted with a full collection of the transmitted pulse, and no aperture was used. Experiments with DMF solvent alone afforded no detectable OL effect; this indicated that the solvent contribution was negligible.

Figure 4 represents the OL response for the investigated complex to nanosecond pulses with intensity transmittances of 62%. At very low fluence, the complex sample responds linearly to the incident light fluence obeying Beer's law. The light energy

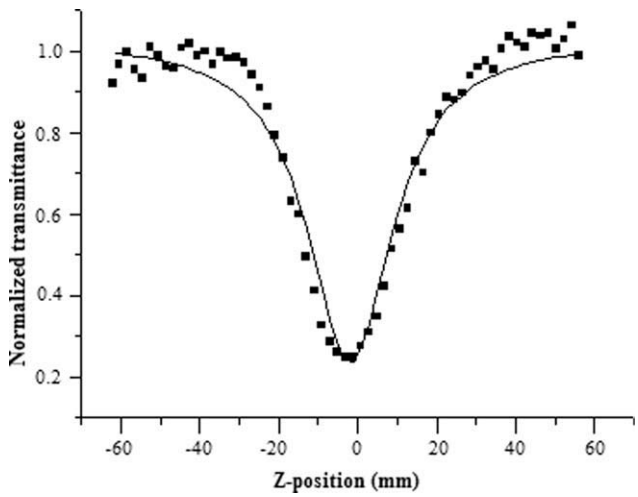

Figure 3 NLO absorptive properties of $\{[Ag_2(pbbt)_3](NO_3)_2{\cdot}0.5H_2O\}_n$ in a 1.4×10^{-4} mol/dm^3 DMF solution at 532 nm ($I_o = 8.2 \times 10^{12}$ W/m^2). The black squares are experimental data, and the solid curve is the theoretical fit.

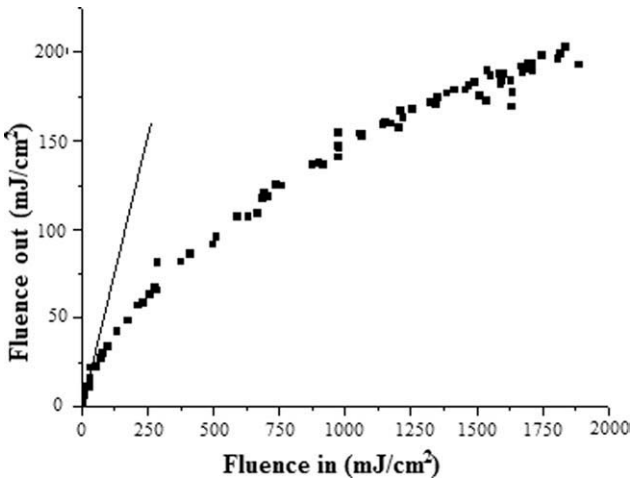

Figure 4 OL effect of $\{[Ag_2(pbbt)_3](NO_3)_2{\cdot}0.5H_2O\}_n$ in a 1.4×10^{-4} mol/dm^3 DMF solution with an 8-ns laser pulse at 532 nm. The straight lines are guides to the eye for the situation where Beer's law is obeyed and with 62%.

transmittance started to deviate from normal linear behavior as soon as the input light fluence reached about 0.04 J/cm^2. The complex sample became increasingly less transparent as the light fluence rose. The *limiting threshold*, defined as the incident fluence at which the actual transmittance falls to 50% of the corresponding linear transmittance, was about 0.16 J/cm^2 of the investigated complex. This value was comparable to those of the well-known OL materials C_{60}–fullerene (0.16–0.19 J/cm^2),[33] phthalocyanine derivatives ($\sim$ 0.1 J/cm^{-2}),[34] and Mo(W)/S/Cu(Ag) clusters (0.07–0.50 J/cm^2).[27]

The picosecond OL ability of the investigated complex was performed under the irradiation of 30-ps laser pulses. The result is depicted in Figure 5. The OL effect appeared around 0.06 J/cm^2 input energy, and above this threshold, there was a strong linear decrease of the transmission versus the fluence. The limiting threshold was measured to be about 0.56 J/cm^2 for the complex with a saturation fluence around 0.2 J/cm^2. It is well known that the higher the electronic polarizability of the metal center is, the shorter the lifetime of the first excited state will be and the higher the yield of formation of the absorbing triplet excited state will be.[35] In the nanosecond case, the metal complexes are well-suited to exhibit rapid and efficient RSA where RSA is reverse saturable absorption,[36,37] and triplet–triplet transitions have been identified as the main mechanism responsible.[38,39] Because the excitation with picosecond laser pulses may result in a relatively small population of the triplet state, the populations of a singlet excited state mainly contributed to the picosecond OL performances.[20,35] Therefore, the investigated complex presented different nanosecond and picosecond OL effects due to different mechanisms. It was similar to the reported Ag cluster $[MS_4Cu_4X_2(py)_6]$ (M = W, Mo; X = I, Br, or Cl)[40] and Ag-bridged polymeric complexes $\{[Ag(bpfp)](NO_3)(H_2O)\}_n$ and $\{[Ag(btx)](NO_3)H_2O\}_n$.[7] Thus far, the silver-containing complexes under investigation as OL materials have included silver clusters,[27] gold–silver alloy nanoclusters,[41] nanocrystalline silver,[42] silver sulfide, and silver bromide nanoparticles,[43] many of which have exhibited large and interesting OL performances. Our studies on a series of Ag(I)-bridged polymeric complexes[7–9] revealed that these complexes increased effective conjugations and large π delocalization lengths because of their polymeric structures and, thus, presented more strong OL effects than other Ag-containing complexes.

The OL effect of the pure ligand pbbt under the same testing conditions as the complex sample was also determined. As we foresaw, the OL of the pure ligand was the same as that of the DMF solvent both toward 8-ns and 30-ps laser pulses because of its hardly third-order nonlinear absorption. This result shows that the pure ligand pbbt hardly contributed to OL effects. Concerning to the strong OL effect of the investigated complex, we concluded that the incorporation of metal ions, especially silver ions, largely enhanced the optical nonlinearities of the attached organic molecules. Furthermore, the generation of acoustic waves by the absorption of light in a liquid medium is known as the *photoacoustic effect*, and the thermal effect appeared in the medium connected with the spreading of the acoustic wave.[44–46] The OL effects of a nanoparticle colloidal solution can also be connected with an acoustic blast wave in a liquid as a result of laser pulse absorption on metal particles in the spot. Thus, the OL effect of the presented complex also included such an acoustic effect.

Theoretical calculation was a powerful tool for explaining the micromechanism of the molecules'

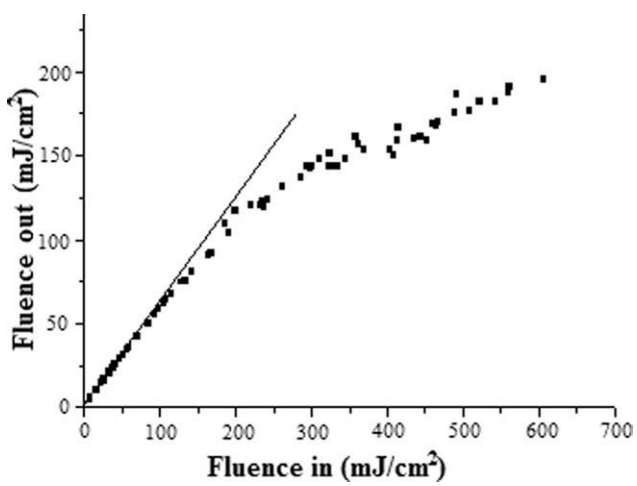

Figure 5 OL effect of $\{[Ag_2(pbbt)_3](NO_3)_2{\cdot}0.5H_2O\}_n$ in a 1.4×10^{-4} mol/dm^3 DMF solution with a 30-ps laser pulse at 532 nm. The straight lines are guides to the eye for the situation where Beer's law is obeyed and with 62%.

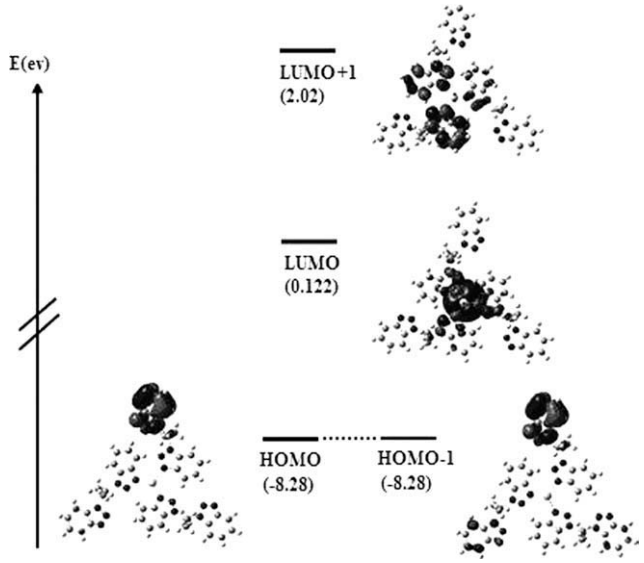

Figure 6 Energies and shapes of the molecular orbitals in $\{[Ag_2(pbbt)_3](NO_3)_2{\cdot}0.5H_2O\}_n$ (Ag represents Ag1A, Ag1B, Ag1C, etc., in Fig. 1).

NLO properties. Because the delocalization was in agreement with the frontier molecular orbital, we could calculate the contributions of metal ions and ligands and deduce the action of metal ions or ligands to the NLO properties by molecular orbital theory. By means of the DFT/B3LYP method, our recent NLO studies revealed that there were main contributions of the center Ag(I) ions on the frontier molecular orbitals in some Ag-containing complexes (strong NLO properties),[7,8] and less metal characteristics were found in the frontier molecular orbitals of Zn(II), Cd(II), and Hg(II) congeners (weak NLO properties).[8,17] These calculation results were very consistent with the experimental facts. Therefore, the DFT/B3LYP method was again employed to in this complex to provide the theoretical basis for understanding the roles of silver ions and the pbbt ligand on the optical nonlinearity properties. The calculation results for the frontier orbital contributions are shown in Figures 6 and S1; these had very similar appearances because Ag1 and Ag2 are two crystallographically independent Ag(I) ions. The contributions of Ag and ppbt to the molecular orbitals were expressed as percentages to the sum of the squares of the atomic orbital coefficient in the $[Ag(pbbt)_3]^+$. In the case of Ag1, it can be seen from Figure 6 that the contribution of Ag atoms in the lowest unoccupied molecular orbital (LUMO) of $[Ag(pbbt)_3]^+$ was 65.67%, and thus, the contributions of pbbt ligand were relatively small (34.33%), whereas the contributions of Ag atoms in LUMO+1, HOMO−1 (where HOMO is the highest occupied molecular orbital), and HOMO of $[Ag(pbbt)_3]^+$ dropped sharply to 0.85, about 0, and about 0%, respectively; this indicated that these frontier molecular orbitals were hardly Ag-based orbitals and were primarily pbbt-based orbitals. Obviously, the LUMO was mainly controlled by both Ag ions and pbbt, whereas HOMO−1, HOMO, and LUMO+1 were controlled by pbbt. Similarly, in the frontier molecular orbitals of $[Ag(pbbt)_3]^+$ with the Ag2 center (Fig. S1), HOMO−1, HOMO, LUMO, and LUMO+1 were about 0, about 0, 65.39%, and 0.80%, respectively, for Ag^+ and about 100%, about 100%, 34.61%, and 99.20%, respectively, for the pbbt ligand. Upon comparing the orbital component of HOMO and LUMO, it was easy to conclude that when electrons were excited from HOMO to LUMO, they mainly transmitted from pbbt ligand to silver center. Because the electron on the HOMO was excited to the LUMO to give rise to the first excited singlet state (S_1) or the first excited triplet state (T_1), the LUMO was regarded to be more responsible for the optical nonlinearity.[47] Therefore, we concluded that the NLO properties of this complex were controlled by Ag(I) ions and the ligand. This was consistent with the experimental facts, namely, that the complex sample displayed enhanced NLO properties with the incorporation of Ag(I) ions.

CONCLUSIONS

In aiming to search for highly efficient limiters and to gain an understanding of Ag-based *N*-heterocyclic complexes in providing exceptional OL responses, we synthesized a novel polymeric Ag(I) complex. Our research revealed that this complex presented fast responses both toward nanosecond and picosecond laser pulses and possessed very strong third-order NLO absorptive properties. The favorable nonlinearity could be attributed to the incorporation of photoactive Ag(I) ions, which permitted the possibility of optimizing the OL properties and enhanced the optical nonlinearities of organic molecules attached. DFT calculation further illustrated that the strong OL capability was mainly due to the contribution of coordinating Ag(I) ions. It can be expected that more studies could improve the OL capabilities of this class through further structural modifications for broadband OL applications.

References

1. Randles, M. D.; Lucas, N. T.; Cifuentes, M. P.; Humphrey, M. G.; Smith, M. K.; Willis, A. C. Macromolecules 2007, 40, 7807.
2. Coe, B. J. In Comprehensive Coordination Chemistry II; McCleverty, J. A., Meyer, T. J., Eds.; Elsevier-Pergamon: Oxford, 2004; Vol. 9, p 621.
3. Jecs, E.; Kreicberga, J.; Kampars, V.; Jurgis, A.; Rutkis, M. Opt Mater 2009, 31, 1600.
4. Pan, H.; Chen, W.; Feng, Y.; Ji, W. Appl Phys Lett 2006, 88, 223106.
5. Webster, S.; Odom, S. A.; Padilha, L. A.; Przhonska, O. V.; Peceli, D.; Hu, H.; Nootz, G.; Kachkovski, A. D.; Matichak, J.;

Barlow, S.; Anderson, H. L.; Marder, S. R.; Hagan, D. J.; Stryland, E. W. V. J Phys Chem B 2009, 113, 14854.
6. Guo, F.; Sun, W. J Phys Chem B 2006, 110, 15029.
7. Xu, H.; Song, Y. L.; Meng, X. R.; Hou, H. W.; Tang, M. S.; Fan, Y. T. Chem Phys 2009, 359, 101.
8. Hou, H. W.; Wei, Y. L.; Song, Y. L.; Mi, L. W.; Tang, M. S.; Li, L. K.; Fan, Y. T. Angew Chem Int Ed Engl 2005, 44, 6221.
9. Niu, Y. Y.; Song, Y. L.; Hou, H. W.; Zhu, Y. Inorg Chem 2005, 44, 2553.
10. Xie, X. J.; Yang, G. S.; Cheng, L.; Wang, F. Huaxue Shiji 2000, 4, 222.
11. Sheldrick, G. M. SHELXL-97, Program for Crystal Structure Solution; Göttingen University: Göttingen, Germany, 1997.
12. Sheik-Bahae, M.; Said, A. A.; Van Stryland, E. W. Opt Lett 1989, 14, 955.
13. Sheik-Bahae, M.; Hutchings, D. C.; Hagan, D. J.; Stryland, E. W. V. IEEE J. Quantum Electron 1991, 27, 1296.
14. Dragonetti, C.; Righetto, S.; Roberto, D.; Ugo, R.; Valore, A.; Fantacci, S.; Sgamellotti, A.; Angelis, F. D. Chem Commun 2007, 4116.
15. Liu, C. G.; Qiu, Y. Q.; Sun, S. L.; Chen, H.; Li, N.; Su, Z. M. Chem Phys Lett 2006, 429, 570.
16. Liu, X. D.; Qiu, Y. Q.; Chen, H.; Li, N.; Sun, S. L.; Su, Z. M. Sci China Ser B Chem 2009, 52, 144.
17. Wu, J.; Song, Y. L.; Zhang, E. P.; Hou, H. W.; Fan, Y. T.; Zhu, Y. Chem—Eur J 2006, 12, 5823.
18. Frisch, M. J. G.; Trucks, W.; Schlegel, H. B.; Scuseria, G. E.; Robb, M. A.; Cheeseman, J. R.; Montgomery, J. A.; Vreven, J. T.; Kudin, K. N.; Burant, J. C.; Millam, J. M.; Iyengar, S. S. Gaussian 03, Revision C.02.; Gaussian; Wallingford, CT, 2004.
19. Hong, M. C.; Su, W. P.; Cao, R.; Fujita, M.; Lu, J. X. Chem—-Eur J 2000, 6, 427.
20. Joshi, H. S.; Jamshidi, R.; Yitzhak, T. Angew Chem Int Ed 1999, 38, 2722.
21. Yam, V. W. W.; Fung, W. K. M.; Cheung, K. K. Chem Commun 1997, 963.
22. Shi, S.; Hou, H. W.; Xin, X. Q. J Phys Chem 1995, 99, 4050.
23. Han, H. Y.; Song, Y. L.; Hou, H. W.; Fan, Y. T.; Zhu, Y. Dalton Trans 2006, 1972.
24. Xu, H.; Song, Y. L.; Mi, L. W.; Hou, H. W.; Tang, M. S.; Sang, Y. L.; Fan, Y. T.; Pan, Y. Dalton Trans 2006, 838.
25. Egorov, A. N.; Mavritsky, O. B.; Petrovsky, A. N.; Yakubovsky, K. V. Laser Phys 1995, 5, 1006.
26. Bredas, J. L.; Adant, C.; Tackx, P.; Persoons, A.; Pierce, B. M. Chem Rev 1994, 94, 243.
27. Zhang, C.; Song, Y. L.; Wang, X. Coord Chem Rev 2007, 251, 111.
28. Meng, X. R.; Song, Y. L.; Hou, H. W.; Fan, Y. T.; Zhu, Y. Inorg Chem 2003, 42, 1306.
29. Meng, X. R.; Li, J. P.; Hou, H. W.; Song, Y. L.; Fan, Y. T.; Zhou, Y. J Mol Struct 2008, 891, 305.
30. Yam, V. W. W. Acc Chem Res 2002, 35, 555.
31. Liu, W.; Jiao, T.; Li, Y.; Liu, Q.; Tan, M.; Wang, H.; Wang, L. J Am Chem Soc 2004, 126, 2280.
32. Calvete, M.; Yang, G. Y.; Hanack, M. Synth Met 2004, 141, 231.
33. Zheng, S. L.; Zhang, J. P.; Wong, W. T.; Chen, X. M. J Am Chem Soc 2003, 125, 6882.
34. Kaneti, J.; de Smet, L. C. P. M.; Boom, R.; Zuilhof, H.; Sudhölter, E. J. R. J Phys Chem A 2002, 106, 11197.
35. Zhang, C.; Song, Y. L.; Kühn, F. E.; Wang, Y. X.; Xin, X. Q.; Herrmann, W. A. Adv Mater 2002, 14, 818.
36. Tom, R. T.; Nair, A. S.; Singh, N.; Aslam, M.; Nagendra, C. L.; Philip, R.; Vijayamohanan, K.; Pradeep, T. Langmuir 2003, 19, 3439.
37. Hollins, R. C.; Opin, C. Solid State Mater Sci 1999, 4, 189.
38. Liu, C.; Wang, X.; Gong, Q.; Tang, K.; Jin, X.; Yan, H.; Cui, P. Adv Mater 2001, 13, 1687.
39. Henari, F.; Callaghan, J.; Stiel, H.; Blau, W.; Cardin, D. J Chem Phys Lett 1992, 199, 144.
40. Sahyun, M. R. V.; Hill, S. E.; Serpone, N.; Danesh, R.; Sharma, D. K. J Appl Phys 1996, 79, 8030.
41. Zhang, H.; Zelmon, D. E.; Deng, L.; Liu, H. K.; Teo, B. K. J Am Chem Soc 2001, 123, 11300.
42. Sun, Y. P.; Riggs, J. E.; Rollins, H. W.; Guduru, R. J Phys Chem B 1999, 103, 77.
43. Ispasoiu, R. G.; Balogh, L.; Varnavski, O. P.; Tomalia, D. A.; Goodson, T. G. J Am Chem Soc 2000, 122, 11005.
44. Ravishankar, S. R.; Jones, B. E. NDT E Int 2007, 40, 602.
45. Ganeev, R. A.; Ryasnyansky, A. I.; Kodirov, M. K.; Kamalov, S. R.; Li, V. A.; Tugushev, R. I.; Usmanov, T. Appl Phys B 2002, 74, 47.
46. Joudrier, V.; Bourdon, P.; Hache, F.; Flytzanis, C. Appl Phys B 1998, 67, 627.
47. Chen, Y. S.; Wang, Y. X.; Ye, S. Int J Quantum Chem 2005, 103, 60.